

Estimation of seismic attenuation of gas hydrate bearing sediments from multi-channel seismic data: A case study from Krishna-Godavari offshore basin

Dewangan, P.^{1*}, Mandal¹, R., Jaiswal², P., Ramprasad, T.¹, Sriram, G.¹

¹ CSIR-National Institute of Oceanography, Dona Paula, Goa, 403004, India

² Boone Pickens School of Geology, Oklahoma State University, Stillwater, Oklahoma 74078, USA

*Corresponding author email: pdewangan@nio.org

Abstract

Seismic attenuation of gas hydrate bearing sediments is estimated from the multi-channel seismic data acquired in Krishna-Godavari (KG) offshore basin in the vicinity of Site NGHP-01-10, where ~128 m of fracture-filled hydrate is confirmed by drilling/coring, to understand the effect of gas hydrate on the seismic attenuation. The seismic quality factor (Q), which is the inverse of seismic attenuation, is estimated from two methods – first, the spectral ratio method which utilizes the logarithmic ratio of the seafloor and bottom simulating reflector (BSR) spectra; and second, the peak frequency method which depends upon the variations of the peak frequency of the BSR spectrum as a function of traveltime. In the study area, the complex fault system has perturbed the seafloor resulting in noisy seafloor spectrum. As a result, the logarithm of the spectral ratio was also noisy and the Q-values obtained from spectral ratio method were found to be unstable. On the other hand, the peak frequency method is found to be relatively stable as it depends only on the peak frequency of the BSR which can be reliably obtained by conventional processing. This method yields an effective Q value of BSR which represents a weighted average of the interval Q-values of the water column and the gas hydrate bearing sediments. Since the Q-value of water column can be treated as a constant, the variations in effective Q-value can be interpreted in terms of the variations of Q in the gas hydrate bearing sediments for a constant thickness of water column. The estimated effective Q-values, along the inline and crossline seismic profiles, depend on several factors such as gas hydrate, free gas and the complex fault system. The combined interpretation of the quality factor and the interval velocity model helps to understand these effects in different zones of the seismic data. The attenuation of the background marine sediments is estimated from the analysis of crossline seismic profile. The gas hydrate bearing sediments, as inferred from the velocity model, show low attenuation as compared to that of the background sediments. In contrast, active migration of free gas across the fault system leads to increase in seismic attenuation within the gas hydrate stability zone. The complex fault zone may also lead to an increase in seismic attenuation. The blanked seismic zone shows a marginal decrease in seismic attenuation probably related to load-bearing form of gas hydrate. Our attenuation results are compared against the results obtained from waveform inversion, albeit with a higher resolution. The relative variation of Q estimated from the proposed method is close to the average Q-values estimated from full waveform inversion for most of the CDPs. The proposed methodology can be a useful technique to estimate seismic attenuation from multi-channel seismic data.

Keywords: gas hydrate, seismic attenuation, peak frequency method, spectral ratio, bottom simulating reflector (BSR)

1. Introduction

Gas hydrate is a ice-like, non-stoichiometric, crystalline solid formed under high pressures and low temperatures when the gas concentration exceeds the solubility limit (Sloan, 1998). Gas hydrate is widely present in continental slope environments (Kvenvolden, 1988) where thick water column exerts adequate pressure to stabilize the gas hydrate. The occurrence of gas hydrates can be inferred from the presence of bottom simulating reflectors (BSRs) in the multi-channel seismic (MCS) data. BSR is manifested in the seismic data due to the impedance contrast between the overlying gas hydrate bearing sediments and underlying free gas bearing sediments. BSR is identified in the seismic profile based on its characteristics properties: i) mimicking the sea-floor topography, ii) opposite polarity with respect to ocean bottom, and iii) crosscut the existing geological horizons since the BSR represents a phase transition (e.g., Markl et al., 1970; Shipley et al., 1979; Hyndman and Spence, 1992). Seismic studies on several active and passive margins demonstrate that the high amplitude BSR is primarily due to the presence of free gas at the base of the gas hydrate stability zone (e.g., Bangs et al., 1993; Mackay et al., 1994; Singh et al., 1993; Holbrook et al., 1996).

The effect of gas hydrate on seismic velocities is well known; it tends to increase both P- and S-wave velocities of the marine sediments with increase in hydrate concentration. However, the magnitude of velocity increase depends on the type and distribution of gas hydrate within the host sediments. Several rock physics models like the cementation theory (Ecker et al., 1998), effective medium model (EMM; Helgerud et al., 1999), self-consistent approximation (SCA) and differential effective medium (DEM) (Jakobsen et al., 2000), three-phase Biot type equation (TPBE; Carcione and Tinivella, 2000; Lee and Waite, 2008) are formulated to understand the increase in velocity for a particular distribution of gas hydrate. In contrast, attenuation trends in the gas hydrate bearing sediments are still actively debated. Pecher and Holbrook (2003) suggested that cementing form of hydrate can increase attenuation, but Rossi et al. (2007) suggested that cementing hydrate may decrease attenuation based on the analysis of 3D seismic data from western Svalbard. The analysis of sonic waveform from Mallik 2L-38 gas hydrate research well, Mackenzie delta, Canada shows that the presence of hydrate increases attenuation (Guerin and Goldberg, 2002). The P-wave quality factor estimated from vertical seismic profiling (VSP) data at Mallik shows significant attenuation of gas hydrate bearing sediments (Bellefleur et al., 2007). However, Lee (2006) argued that the apparent increase in seismic attenuation at Mallik site was due to source-coupling and may not be related to the presence of gas hydrate. Laboratory measurements on synthetic methane hydrate bearing sand at seismic frequencies (50-500 Hz) show that

attenuation increases non-linearly with increase in hydrate concentration (Best et al., 2013; Priest et al., 2006). The time lapse crosshole seismic experiment at Mallik field sites shows that the high velocity gas hydrate bearing layers are also associated with high attenuation (Pratt et al., 2005). However, the vertical seismic profiling (VSP) experiment from the Nankai trough exploratory well shows no significant seismic attenuation for methane-hydrate bearing sediments (Matsushima, 2006). In contrast, Sain et al. (2009) argued that the presence of gas hydrate act as cement and gives strength to the host sediment which leads to the decrease in attenuation in the seismic frequency band. Clearly, the effect of gas hydrate on seismic attenuation seems to vary from region-to-region and also from experiment-to-experiment within the same region. Theoretically, the presence of hydrate strengthens the sediment with the increase in bulk and shear modulus; hence it is expected that the attenuation should decrease with hydrate saturation. Alternatively, the increase in seismic attenuation of gas hydrate bearing sediment may be explained by the energy loss mechanism involving the fluid flows within the pores of hydrate matrix (Chand and Minshull, 2004).

Drilling/coring has confirmed the presence of gas hydrate in Krishna-Godavari offshore basin, Bay of Bengal (Fig. 1). One of the drilled sites, NGHP-01-10 shows significant accumulation of gas hydrate which is primarily controlled by fractures (Lee and Collett, 2009). The analysis of high resolution multichannel seismic data in the vicinity of Site NGHP-01-10 show regional fault system and geothermal gradient increases by 15-20 % at Site NGHP-01-10 as compared to the background geothermal gradient due to the migration of deeply-originating fluid through the fault system (Dewangan et al., 2011). The P-wave velocity estimated from unified imaging in the vicinity of Site NGHP-01-10 shows heterogeneous and patchy distribution of gas hydrate which maintains its continuity along strike of the regional fault system (Jaiswal et al., 2012a). The P-wave quality factor estimated from full-waveform inversion shows that free gas enhances attenuation while the presence of hydrate decreases seismic attenuation (Jaiswal et al., 2012b). Full-waveform inversion, as used by Jaiswal et al. (2012b) depends on data preconditioning as well as on the starting model. The starting attenuation model in Jaiswal et al. (2012b) was a simplistic, zero-attenuation subsurface. In the present study, we evaluated the well-known methods such as spectral-ratio method (Båth, 1982) and peak frequency approach (Zhang and Ulrych, 2002) for their suitability in estimating seismic attenuation from multi-channel seismic data in KG offshore basin. Our 1D results are compared with that obtained from full-waveform inversion along a inline seismic profile to understand the effect of hydrate, free gas and complex fault pattern towards seismic attenuation. The same method is applied to a crossline seismic

profile to demonstrate the applicability of the method towards the estimation of seismic attenuation from multi-channel seismic data.

2. Theory

A seismic wave travelling through the medium experiences absorption, spreading loss and dispersion due to which the wave loses its amplitude as it propagates. The main processes which lead to loss of seismic amplitude are as follows: geometric spreading, scattering and intrinsic attenuation. The first two processes can be explained by elastic wave theory; however the third process i.e., intrinsic attenuation is explained by inelasticity / poro-elastic wave theory. Intrinsic attenuation is defined as the loss in seismic amplitude as the wave propagates through the poro-elastic / visco-elastic medium due to the conversion of mechanical energy into thermal energy. The loss of energy due to intrinsic attenuation can be quantified using absorption coefficient (α) which is mathematically defined as an exponential decay of the amplitude of seismic wave with time (τ) as it travels through an inelastic homogeneous medium (Aki and Richards, 1980),

$$A = A_0 e^{-\alpha R} \quad , \quad (1)$$

where, A is the amplitude of seismic wave at distance R and A_0 is the starting amplitude of wave at the origin ($R=0$). The loss of seismic amplitudes can be quantified either with the absorption coefficient (α) or with the help of quality factor (Q) which represents the ratio of the total elastic energy (E) to the energy lost in one cycle (δE) due to attenuation,

$$Q = \frac{2\pi E}{\delta E} \quad . \quad (2)$$

The relationship between the absorption coefficient and the quality factor (Q) is defined as,

$$Q = \frac{\pi}{\alpha \lambda} \quad (3)$$

Attenuation is strongly frequency dependent especially for low Q material. However, over the seismic frequency band (20-150 Hz), Q may be considered as independent of frequency even for unconsolidated marine sediments. In the present study, the loss in seismic amplitude due to scattering is ignored.

Tonn (1991) has compared different quantitative methods for the computation of quality factor from VSP and crosswell data. The estimated quality can be used to nullify the effect of attenuation by

applying inverse Q -filters or can also be recognized as a geological parameter which may improve the understanding of lithology and can aid in the interpretation of seismic sections. One of the best methods for estimating Q is the spectral ratio method (Båth, 1982). In this method, the ratio of the amplitude spectra of a reference signal at depth x_1 and a signal at depth x_2 are computed. The spectral ratio method can be expressed as,

$$\ln\left[\frac{|A(\omega)_2|}{|A(\omega)_1|}\right] = \ln\left[\frac{|A_0(\omega)_2|}{|A_0(\omega)_1|}\right] - m\omega \quad (4)$$

where m is the slope of the linear equation. The quality factor Q can be estimated from the slope (m) as,

$$Q = -\frac{2}{m} \quad (5)$$

The spectral ratio method assumes that the incidence wave is travelling through a homogeneous absorbing media. The spectrum of the signal is assumed to be free from the interference effect and the intercept term incorporates the effect of geometrical spreading and reflection/transmission at the boundaries.

3. Seismic data and Methodology for the estimation of seismic quality factor (Q)

The multi-channel seismic (MCS) data were originally acquired by the Oil and Natural Gas Commission Ltd, and made available to National Institute of Oceanography under National Gas Hydrate Program (NGHP) for estimating seismic attenuation of gas hydrate bearing sediments. The air-gun source was fired at 12.5 m shot spacing, and seismic data were recorded using 1.5 km long hydrophone streamer at 12.5 m group interval. The data was recorded at a 1 ms sample interval with a 4s record length after applying a high cut anti-alias filter of 500 Hz. The nearest source-receiver offset is ~75 m. The raw MCS data was processed to produce a time-migrated seismic section using standard ProMAX data processing routine (c.f., Dewangan et al., 2011). The BSR is identified on the seismic profile based on its characteristics properties. In the present study, two profiles are used for the estimation of seismic attenuation of gas hydrate bearing sediment. The seismic profile oriented in the NW-SE direction will be referred to as inline seismic profile and the profile oriented in the NE-SW direction will be referred to as crossline seismic profile.

The raw seismic data was prepared for estimation of Q using the following processing sequence. In the preprocessing steps, a Butterworth bandpass filter (5-10-200-250 Hz) was applied followed by spherical divergence correction to correct for geometrical spreading. An F-K filter was applied to the

data to remove the effect of random noise from the seismic data and to minimize the effect of interference from the dipping layers reflections on the water bottom reflection and the BSR. The wavelets corresponding to the water bottom and the BSR are extracted on the prestack gather without normal-moveout (NMO) correction. Applying NMO correction will distort the frequency spectrum due to the effect of NMO stretching. In addition, a rectangular hamming window is applied to the extracted wavelet to avoid edge effects in the calculation of spectrum. The frequency spectrum of water bottom and BSR are calculated using fast Fourier transform, and the linear slope in the logarithmic ratio of BSR to seafloor spectrum is used to estimate the Q (equation 6; Dasgupta and Clark, 1998). In the present study, the spectral ratio method produces unstable Q-values in the zones of interest due to the following reasons: a) the diffraction arising from the observed fault systems in KG offshore basin (Dewangan et al., 2011) interfere with the seafloor reflection to produce a noisy seafloor spectrum; b) the frequency spectrum of low amplitude BSR is not reliable over the entire frequency band, and only the dominant frequency can be reliably extracted from the reflection of BSR; c) The logarithm of the spectral ratio does not vary linearly with frequency as expected from the theory and therefore, the estimated Q value becomes dependent on the choice of the frequency band.

In order to overcome these problems, we followed the approach of Zhang and Ulrych (2002) to estimate the attenuation of gas hydrate bearing sediments (Appendix A). In this method, the effective Q can be estimated from the variation of the dominant frequency of BSR with offset/time (equation A4) under the assumption that the source wavelet can be represented by a Ricker wavelet,

$$f_p = f_m^2 \left[\sqrt{\left(\frac{\pi t}{4Q}\right)^2 + \frac{1}{f_m^2}} - \frac{\pi t}{4Q} \right], \quad (6)$$

where f_m represents the initial dominant frequency at the onset of source and f_p represents the dominant frequency of the event at time t . In the case of a CMP gather, f_p can be expressed as a function of time corresponding to different offsets, and both the initial dominant frequency and the quality factor can be estimated using least square approach. The illustrated method can overcome the limitation of conventional spectral ratio method because of the following reasons: a) the method is dependent on only the BSR reflections and therefore, the problem associated with the disturbed seafloor reflections is avoided; b) the method depends only on the peak frequency which can be reliably estimated from the seismic data; c) the method does not depend on the range of frequencies to estimate Q and hence, no a priori information is required.

3.1 Equivalence between the spectral ratio and peak frequency methods

In this section, we attempt to establish the relationship between the seemingly different the spectral ratio and peak frequency methods. Let us assume that the amplitude spectrum $B(f)$ of the reflection after propagating for t sec can be expressed in terms of a Ricker wavelet with dominant frequency f_p ,

$$B_1(f) = \frac{2}{\sqrt{\pi}} \frac{f^2}{f_p^2} e^{-\frac{f^2}{f_p^2}} \quad (7)$$

The amplitude spectrum can also be expressed in terms of the quality factor Q and the propagation time t , $B(f,t)$ [equation (A2)]. The amplitude spectrum of the wavelet at the initiation of source $B(f)$ is given by equation (A1). In spectral ratio method, Q is estimated by the logarithmic ratio of the amplitude spectrum at time $t=0$ and t as,

$$\ln \left[\frac{B(f)}{B(f,t)} \right] = \ln \left[\frac{B(f)}{B_1(f)} \right] = \frac{\pi f t}{Q}. \quad (8)$$

Substituting the expression for $B(f)$ from equation (A1) and $B_1(f)$ from equation (7) leads to ,

$$\ln \left(\frac{f_p^2}{f_m^2} \right) + f^2 \left(\frac{1}{f_p^2} - \frac{1}{f_m^2} \right) - \frac{\pi f t}{Q} = 0 \quad (9)$$

The slope in the log-spectral ratio method can be estimated by differentiating equation (9) with respect to frequency,

$$2f \left(\frac{1}{f_p^2} - \frac{1}{f_m^2} \right) - \frac{\pi t}{Q} = 0. \quad (10)$$

Let's evaluate the slope in the vicinity of the peak frequency,

$$\lim_{f \rightarrow f_p} 2f \left(\frac{f_m^2 - f_p^2}{f_p^2 f_m^2} \right) - \frac{\pi t}{Q} = 0. \quad (11)$$

After evaluating the limit, and further simplifying the results we get,

$$\frac{2}{f_m} - \frac{2}{f_m} \left(\frac{f_p^2}{f_m^2} \right) - \frac{\pi t}{Q} \left(\frac{f_p}{f_m} \right) = 0. \quad (12)$$

One of the solutions of the quadratic equation is,

$$f_p = f_m^2 \left[\sqrt{\left(\frac{\pi t}{4Q}\right)^2 + \frac{1}{f_m^2}} - \frac{\pi t}{4Q} \right], \quad (13)$$

which is exactly same as equation (6) of peak frequency method (Zhang and Ulrych, 2002). Thus, the peak frequency method is equivalent to the spectral ratio method under the assumption that the wavelet can be locally approximated by a Ricker wavelet and the slope of the log-spectral ratio is evaluated in the vicinity of the peak frequency.

4. Results

The processed time-migrated seismic sections (Figs. 2a and 3a) show the presence of BSR in the inline and crossline profiles. The BSR is identified based on its characteristic properties such as mimicking the seafloor topography and crosscutting the existing geological reflectors. The seafloor and BSR zero-offset traveltimes were picked on the time-migrated seismic section. The traveltimes at other offsets are calculated from hyperbolic normal moveout equation (NMO) using the velocity model estimated from conventional semblance analysis (Dewangan et al., 2011). In order to illustrate the peak-frequency method, three representative gathers of the inline profile at common depth point (CDP) 392, 672 and 710 are shown in Figure 2b. Likewise, three representative gathers of the crossline profile at CDPs 448, 590, and 765 are shown in Figure 3b. The calculated traveltimes of both the seafloor and the BSR match well with the observed traveltimes. The BSR wavelet is windowed and its edges are rounded; the spectrum of BSR is computed using fast Fourier transform. The peak frequency of the spectrum is estimated as a function of offset/traveltime and is shown as black circles in Figure 4. The peak frequency decreases systematically with offset showing the effect of seismic attenuation. The quality factor (Q) and the initial frequency (f_m) are estimated by fitting the peak frequency with the pattern predicted by equation (6) using constrained non-linear optimization (Xue and Chen, 2011). If the peak frequency of the BSR is either too high or too low due to interference effect, it is discarded from the estimation process to improve the reliability of the solution. The estimated Q -value represents the effective Q value which has contribution from both the water column and gas hydrate bearing sediments. The apparent interval Q values can be obtained from the effective Q using a Dix-type formula and represents the time weighted harmonic average of interval Q values along the ray path [eq. 31; Zhang and Ulrych, 2002]. The methodology is repeated for all CDPs to estimate the variations in Q -values along the seismic profile. Due to the interference effect from the other geological reflectors,

rigorous quality control measures are needed to assess the reliability of Q-values. The estimated Q values were considered to be unreliable under the following conditions: a) if the amplitudes of BSR are small; b) the BSR is difficult to be identified in the prestack gather; c) the dominant frequency does not decrease or increases with offset; d) the error between the observed and modeled peak frequency is higher than the specified tolerance level. In addition, the estimated Q values should show consistency for a range of nearby CDPs. If the Q values show large fluctuations for nearby CDPs, it is again considered to be unreliable.

The estimated effective Q-values are shown for the inline seismic profile in Figure 5a and interpreted seismic section is shown in Figure 5b. The effective Q values of the gas hydrate bearing sediments fluctuate between 160 and 320. The background Q of marine sediments is estimated to be ~230-240 from the crossline seismic profile where the presence of gas hydrate is almost negligible as inferred from its velocity model. High Q-values (260-300) are observed around CDP 400 in the vicinity of major fault system F1, from CDPs 520-670 in between the fault systems F1 and F2 and from CDPs 710-720 in between the fault systems F1 and F2 (Fig. 5). Moderate Q-values (240-260) are observed in the vicinity of fault F2 and around CDPs 830-900 in the vicinity of observed blanked zone in the seismic section (Fig. 5b). In contrast, low Q-values (< 240) are observed around CDP 470 across the major fault system F1 and also around CDP 760 in the vicinity of fault F3. No reliable estimate of Q is ascertained between CDPs 200 and 350 as it is difficult to identify the BSR in the prestack gathers.

The estimated effective Q-value and interpreted crossline seismic profile are shown in Figure 6a and 6b, respectively. The BSR is identified in the seismic section from CDPs 400 to 800. Beyond CDP No. 800, BSR identification is doubtful as cross cutting feature is not observed. Several faults are interpreted between CDPs 600 and 800. High quality factor (~300) is observed in the vicinity of CDP no. 600 and moderate Q-values are observed between CDPs 630 and 775. A constant Q (230-240) is observed for a range of CDPs from 440-550. Low Q-value (~ 200) is observed in the vicinity of CDP 400.

5. Discussion

The mechanism of intrinsic attenuation, which explains the observed loss of seismic amplitudes, can be broadly classified into three categories: matrix inelasticity, viscosity and flow of pore fluids, and partial saturation by two or more fluids (Johnston et al., 1979; Toksöz et al., 1979). Each mechanism is independent, and overall attenuation may occur due to the combination of one or more mechanisms. The presence of gas hydrate, free gas, complex fault system or patchy saturation of both hydrate and free gas

may influence the seismic attenuation in the present study. It is difficult to decouple the effect of these factors from the estimated Q-values, but the combined interpretation of velocity model and structural features can help in localizing the zones where a particular factor is more dominant than the others.

5.1 Seismic attenuation of gas hydrate bearing sediments

The presence of gas hydrate increases the velocity of marine sediments. Depending on the form and distribution of gas hydrate, the gas hydrate bearing sediments may show slight increase in velocities for the hydrate within the pore spaces, moderate increase for load bearing hydrate, or rapid increase for the hydrate acting as intra-granular cement (Helgerud et al., 1999). On the other hand, the presence of free gas leads to dramatic decreases in the seismic velocity (White, 1975). In contrast, the effect of gas hydrate on seismic attenuation in marine sediments is poorly understood. One of the key factors in understanding the attenuation of gas hydrate bearing sediments is the attenuation of the background marine sediments. The analysis of log data at Site NGHP-01-10 suggests that the background velocity of marine sediments is ~ 1.55 - 1.6 km/s (Lee and Collett., 2009). In the crossline seismic profile, a range of CDPs from 440 to 550 show velocities similar to the background velocity in KG offshore basin. The estimate effective Q for these CDPs ranges from 230-240. Therefore, we have considered a Q value of 230-240 to be the background Q of the marine sediments.

The inverse of Q values (Q^{-1} is directly proportional to seismic attenuation) as estimated from the peak-frequency method and the velocity and attenuation models as estimated from the full waveform inversion (Jaiswal et al., 2012b) are shown in Figure 7a, 7b and 7c, respectively to understand the primary process responsible for the seismic attenuation in marine sediments. The interval P-wave velocity derived from unified imaging (Jaiswal et al., 2012a), and later refined from waveform inversion (Jaiswal et al., 2012b) shows several local patches of high velocity ($V_p > 1.7$ km/s) indicating hydrate-bearing sediments (Fig. 7b). Interestingly, the high velocity patch around CDPs 400, 520- 670 shows low Q^{-1} values (Fig. 7a) suggesting that the gas hydrate bearing sediments have lower attenuation than that of the background marine sediments. Low-to-moderate seismic attenuation is observed in the vicinity of Site NGHP-01-10 (CDP 725) where ~ 128 m of thick gas hydrate is confirmed by drilling/coring onboard JOIDES Resolution (Collett et al., 2008). The detailed interval attenuation model (Fig. 7c) derived from an independent technique, full waveform inversion, also support the hypothesis of lower attenuation for gas hydrate bearing sediments (Jaiswal et al., 2012b). This hypothesis of further supported by the analysis of the crossline seismic profile (Fig. 6) where high-to-

moderate Q values are observed from CDPs 590 to 775 corresponding to high velocity patch. Similar reduction in seismic attenuation due to the presence of gas hydrate is also observed for low-permeability (e.g., clay-dominated) medium in offshore NW Svalbard (Rossi et al., 2007) and Blake ridge (Wood et al., 2000).

5.2 Seismic attenuation due to fluid migration and heavily faulted zone

The presence of free gas leads to dramatic decrease in P-wave velocity and increase in seismic attenuation (White, 1975). Low velocity anomaly is observed throughout the seismic profile immediately below the base of gas hydrate stability zone (GHSZ) suggesting the presence of thick gas layer (Fig. 7b). The drop in dominant frequency as observed in the seismic data (Figs. 2a and 3a) for the free-gas bearing horizon suggests significant attenuation due to free gas which is also confirmed from the result of waveform inversion (Jaiswal et al., 2012b). Within GHSZ, the P-wave velocity is below the threshold velocity of marine sediments (< 1.6 km/s) across the fault F1. The seismic attenuation increases slightly across the fault F1. We interpret the decrease in velocity and increase in attenuation to be related to the migration of fluid/free gas within the GHSZ which is known to exist in KG offshore basin (Dewangan et al., 2011).

Regional fault systems, probably controlled by shale tectonism/neotectonic activity, are observed in KG offshore basin (Dewangan et al., 2010, 2011; Ramprasad et al., 2011; Riedel et al., 2010). These faults may have facilitated the movement of fluid/gas into the hydrate stability zone. The seismic attenuation is compared against the observed faults pattern, as interpreted by Jaiswal et al. (2012b), along the inline seismic profile (Fig. 7c). A significant increase in seismic attenuation is observed at the center of complex fault pattern (F2 – F4 zone) in the vicinity of the fault F3. The attenuation estimated using waveform inversion also shows a similar increase in attenuation within this heavily faulted zone. The likely mechanism for the increase in seismic attenuation is the migration of fluid through the complex fault pattern.

Amplitude blanking associated with high velocity anomaly (> 1.7 km/s; Fig. 7b) is observed in the vicinity of CDP 900 along the inline seismic profile (Fig. 5b) suggesting the presence of gas hydrate. The estimated Q^{-1} values are marginally low for this blanked zone suggesting that the gas hydrate bearing sediments have lower attenuation than the background sediment. However, the identification of BSR in the prestack gather is doubtful in this zone limiting the reliability of the results. A detailed investigation

is warranted to understand the form and distribution of hydrate in the blanked zone, and its relationship with seismic attenuation.

6. Conclusions

A couple of the well known methods are evaluated for their applicability in estimating seismic quality factor (Q) from seismic data in KG offshore basin. The widely used spectral ratio method gave inconsistent results as the spectrum of the seafloor is noisy owing to the perturbation in seafloor due to fault system. We adopted an alternative method in which the effective-Q is estimated only from the variation of peak frequency of BSR with offset. A stringent quality control measures on the estimated Q values provide a reliable, unbiased estimate of effective Q. The relative variation of the effective Q along with the interval velocity model is used to understand the effect of gas hydrate, free gas and complex fault system on seismic attenuation. The zones of gas hydrate, identified by the increase in seismic velocity, show elevated Q-values indicating that the presence of hydrate decreases attenuation in fine grained, clay dominated marine sediments. The presence of free gas within the gas hydrate stability zone across the fault F1 leads to increase in seismic attenuation. The complex fault system in the vicinity of fault F3 also shows a prominent increase in seismic attenuation probably due to the migration of free gas through the fault system. In contrast, the blanked zone in seismic section shows a marginal decrease in seismic attenuation probably due to the presence of load-bearing gas hydrate. The interpretation derived from the relative variation of effective Q is largely consistent with that inferred from the results of waveform inversion. Therefore, the methodology involving only the peak frequency of BSR may be used as a technique for estimating effective Q values from the multi-channel seismic data.

Acknowledgements

The authors wish to thank those that contributed to the success of the National Gas Hydrate Program Expedition 01 (NGHP-01). NGHP-01 was planned and managed through collaboration between the Directorate General of Hydrocarbons (DGH) under the Ministry of Petroleum and Natural Gas (India), the U.S. Geological Survey (USGS), and the Consortium for Scientific Methane Hydrate Investigations (CSMHI) led by Overseas Drilling Limited (ODL) and FUGRO McClelland Marine Geosciences (FUGRO). The platform for the drilling operation was the research drill ship *JOIDES Resolution*, operated by ODL. Much of the drilling/coring equipment used was provided by the Integrated Ocean Drilling Program (IODP) through a loan agreement with the US National Science Foundation. Wireline pressure coring systems and supporting laboratories were provided by IODP/Texas A&M University (TAMU), FUGRO, USGS, U.S. Department of Energy (USDOE) and HYACINTH/GeoTek. Downhole logging operational and technical support was provided by Lamont-Doherty Earth Observatory (LDEO) of Columbia University. The financial support for the NGHP-01, from the Oil Industry Development

Board, Oil and Natural Gas Corporation Ltd., GAIL (India) Ltd. and Oil India Ltd. is gratefully acknowledged. We also acknowledge the support extended by all the participating organizations of the NGHP: MoP&NG, DGH, ONGC, GAIL, OIL, NIO, NIOT, and RIL. We thank the Director of CSIR-National Institute of Oceanography (NIO) for supporting this study. We thank ONGC for providing valuable seismic data. We thank A. V. Sathe (ONGC), M. V. Lall (DGH), K. Vishwanath (DGH) and B. J. P. Kumar (DGH) for providing useful comments/suggestions for improving the quality of the manuscript. We would also like to thank two anonymous reviewers for providing useful comments/suggestions which has improved the quality of the manuscript. This is NIO contribution no. xxx.

Appendix A: Peak frequency method (Zhang and Ulrych, 2002)

The propagating wavelet at the onset of source ($t=0$) can be approximated by a Ricker wavelet with dominant frequency f_m as,

$$B(f) = \frac{2}{\sqrt{\pi}} \frac{f^2}{f_m^2} e^{-\frac{f^2}{f_m^2}} \quad (\text{A1})$$

The amplitude spectrum $B(f,t)$ of the reflection after propagating for t sec can be expressed as,

$$B(f,t) = B(f) e^{-\frac{\pi t}{Q}} \quad (\text{A2})$$

where Q is the quality factor of the medium; f_p is the peak frequency of the wavelet representing the maximum amplitude in the spectral domain. By definition, the peak frequency of BSR reflection at time t sec can be computed by taking derivative of equation (A2) and equating it to zero,

$$\frac{\partial}{\partial f} [B(f,t)] = 0 \Rightarrow f = f_p \quad (\text{A3})$$

Substituting the derivative of $B(f,t)$ from equations (A1) and (A2), and expressing the peak frequency as a function of time,

$$f_p = f_m^2 \left[\sqrt{\left(\frac{\pi t}{4Q}\right)^2 + \frac{1}{f_m^2}} - \frac{\pi t}{4Q} \right] \quad (\text{A4})$$

References

- Aki, K., Richards, P.G., 1980. Quantitative seismology. Freeman San Francisco.
- Bangs, N.J.B., Sawyer, D.S., Golovchenko, X., 1993. Free gas at the base of the gas hydrate zone in the vicinity of the Chile triple junction. *Geology* 21, 905–908.
- Båth, B.M., 1982. Spectral analysis in geophysics. Elsevier Science. 579 pp.
- Bellefleur, G., Riedel, M., Brent, T., Wright, F., Dallimore, S.R., 2007. Implication of seismic attenuation for gas hydrate resource characterization, Mallik, Mackenzie Delta, Canada. *Journal of Geophysical Research* 112, B10311–B10311.
- Best, A.I., Priest, J. a., Clayton, C.R.I., Rees, E.V.L., 2013. The effect of methane hydrate morphology and water saturation on seismic wave attenuation in sand under shallow sub-seafloor conditions. *Earth and Planetary Science Letters* 368, 78–87.
- Carcione, J.M., Tinivella, U., 2000. Bottom-simulating reflectors: Seismic velocities and AVO effects. *Geophysics* 65, 54–67.
- Chand, S., Minshull, T.A., 2004. The effect of hydrate content on seismic attenuation: A case study for Mallik 2L-38 well data, Mackenzie delta, Canada. *Geophysical Research Letters* 31, L14609–L14609.
- Dasgupta, R., Clark, R. a., 1998. Estimation of Q from surface seismic reflection data. *Geophysics* 63, 2120–2128.
- Dewangan, P., Ramprasad, T., Ramana, M. V, Mazumdar, a., Desa, M., Badesab, F.K., 2010. Seabed morphology and gas venting features in the continental slope region of Krishna–Godavari basin, Bay of Bengal: Implications in gas-hydrate exploration. *Marine and Petroleum Geology* 27, 1628–1641.
- Dewangan, P., Sriram, G., Ramprasad, T., Ramana, M.V., Jaiswal, P., 2011. Fault system and thermal regime in the vicinity of site NGHP-01-10, Krishna–Godavari basin, Bay of Bengal. *Marine and Petroleum Geology* 28, 1899–1914.
- Ecker, C., Dvorkin, J., Nur, A., 1998. Sediments with gas hydrates: Internal structure from seismic AVO. *Geophysics* 63, 1659–1669.
- Guerin, G., Goldberg, D., 2002. Sonic waveform attenuation in gas hydrate-bearing sediments from the Mallik 2L-38 research well, Mackenzie Delta, Canada. *Journal of Geophysical Research* 107.
- Helgerud, M.B., Dvorkin, J., Nur, A., Sakai, A., Collett, T., 1999. Elastic-wave velocity in marine sediments with gas hydrates: Effective medium modeling. *Geophysical Research Letters* 26, 2021–2024.
- Holbrook, W.S., Hoskins, H., Wood, W.T., Stephen, R.A., Lizarralde, D., 1996. Methane Hydrate and free gas on the Blake Ridge from vertical seismic profiling. *Science* 273, 1840–1843.

- Hyndman, R.D., Spence, G.D., 1992. A seismic study of methane hydrate marine bottom simulating reflectors. *Journal of Geophysical Research* 97, 6683.
- Jaiswal, P., Dewangan, P., Ramprasad, T., Zelt, C., 2012a. Seismic characterization of hydrates in faulted, fine-grained sediments of Krishna-Godavari basin: Unified imaging. *Journal of Geophysical Research* 117, B04306.
- Jaiswal, P., Dewangan, P., Ramprasad, T., Zelt, C., 2012b. Seismic characterization of hydrates in faulted, fine-grained sediments of Krishna-Godavari Basin: Full waveform inversion. *Journal of Geophysical Research* 117, B10305.
- Jakobsen, M., Hudson, J.A., Minshull, T.A., Singh, S.C., 2000. Elastic properties of hydrate-bearing sediments using effective medium theory. *Journal of Geophysical Research* 105, 561–577.
- Johnston, D.H., Toksöz, M.N., Timur, A., 1979. Attenuation of seismic waves in dry and saturated rocks: II. Mechanisms. *Geophysics* 44, 691–711.
- Kvenvolden, K.A., 1988. Methane hydrate—a major reservoir of carbon in the shallow geosphere? *Chemical Geology* 71, 41–51.
- Lee, M.W., 2006. Is amplitude loss of sonic waveforms due to intrinsic attenuation or source coupling to the medium? US Department of the Interior US Geological Survey.
- Lee, M.W., Collett, T.S., 2009. Gas hydrate saturations estimated from fractured reservoir at Site NGHP-01-10, Krishna-Godavari Basin, India. *Journal of Geophysical Research* 114, B07102.
- Lee, M.W., Waite, W.F., 2008. Estimating pore-space gas hydrate saturations from well log acoustic data. *Geochemistry, Geophysics, Geosystems* 9, 1-8.
- Mackay, M.E., Jarrard, R.D., Westbrook, G.K., Hyndman, R.D., 1994. Accretionary prism origin of bottom-simulating reflectors : Geophysical evidence from the Cascadia accretionary prism. *Geology* 22, 459–462.
- Markl, R.G., Bryan, G.M., Ewing, J.I., 1970. Structure of the Blake-Bahama outer ridge. *Journal of Geophysical Research* 75, 4539–4555.
- Matsushima, J., 2006. Seismic wave attenuation in methane hydrate-bearing sediments: Vertical seismic profiling data from the Nankai Trough exploratory well, offshore Tokai, central Japan. *Journal of Geophysical Research* 111, B10101–B10101.
- Pecher, I.A., Holbrook, W.S., 2003. Seismic methods for detecting and quantifying marine methane hydrate/free gas reservoirs, in: *Natural Gas Hydrate*. Springer, pp. 275–294.
- Pratt, R.G., Hou, F., Bauer, K., Weber, M., 2005. Waveform tomography images of velocity and inelastic attenuation from the Mallik 2002 crosshole seismic surveys. *Bulletin-Geological Survey of Canada* 1–14.

- Priest, J.A., Best, A.I., Clayton, C.R.I., 2006. Attenuation of seismic waves in methane gas hydrate-bearing sand. *Geophysical Journal International* 164, 149–159.
- Ramprasad, T., Dewangan, P., Ramana, M. V, Mazumdar, A., Karisiddaiah, S.M., Ramya, E.R., Sriram, G., 2011. Evidence of slumping/sliding in Krishna–Godavari offshore basin due to gas/fluid movements. *Marine and Petroleum Geology* 28, 1806–1816.
- Riedel, M., Collett, T.S., Kumar, P., Sathe, A.V, Cook, A., 2010. Seismic imaging of a fractured gas hydrate system in the Krishna–Godavari Basin offshore India. *Marine and Petroleum Geology* 27, 1476–1493.
- Rossi, G., Gei, D., Böhm, G., Madrussani, G., Carcione, J.M., 2007. Attenuation tomography: An application to gas-hydrate and free-gas detection. *Geophysical Prospecting* 55, 655–669.
- Sain, K., Singh, A.K., Thakur, N.K., Khanna, R., 2009. Seismic quality factor observations for gas-hydrate-bearing sediments on the western margin of India. *Marine Geophysical Researches* 30, 137–145.
- Shipley, T.H., Houston, M.H., Buffler, R.T., Shaub, F.J., McMillen, K.J., Ladd, J.W., Worzel, J.L., 1979. Seismic evidence for widespread possible gas hydrate horizons on continental slopes and rises. *AAPG Bull* 63, 2204–2213.
- Singh, S.C., Minshull, T.A., Spence, G.D., 1993. Velocity structure of a gas hydrate reflector. *Science* 260, 204–207.
- Sloan, E.D., 1998. *Clathrate Hydrates of Natural Gases* (second ed.). Marcel Dekker, New York.
- Toksöz, M.N., Johnston, D.H., Timur, A., 1979. Attenuation of seismic waves in dry and saturated rocks: I. Laboratory measurements. *Geophysics* 41, 681–690.
- Tonn, R., 1991. The determination of the seismic quality factor Q from VSP data: a comparison of different computational methods. *Geophysical Prospecting*.
- White, J.E., 1975. Computed seismic speeds and attenuation in rocks with partial gas saturation. *Geophysics* 40, 224–232.
- Wood, W.T., Holbrook, W.S., Hoskins, H., 2000. In situ measurements of P-wave attenuation in the methane hydrate and gas-bearing sediments of the Blake ridge, in: *Proceedings of the Ocean Drilling Program. Scientific Results*. pp. 265–272.
- Xue, D., Chen, Y., 2011. *Solving applied mathematical problems with MATLAB*. CRC Press.
- Zhang, C., Ulrych, T.J., 2002. Estimation of quality factors from CMP records. *Geophysics* 67, 1542–1547.

Figures Caption

- Fig. 1. Location map of the study area in KG offshore. The inset shows the zoom out of the study area. The multi-channel seismic data (inline and crossline) in the vicinity of Site NGHP-01-10 (marked as star), where ~128 m of thick gas hydrates have been confirmed by drilling/coring onboard JOIDES resolution, are used for estimating the seismic attenuation of gas hydrate bearing sediments.
- Fig. 2. A) Time-migrated section of the inline seismic data. The BSR is identified on the seismic data based on its characteristic features. B) Three representative prestack CDP gathers in which the reflections from the seafloor and BSR are identified are highlighted.
- Fig. 3. A) Time-migrated section of the crossline seismic data. The BSR is identified on the seismic data based on its characteristic features. B) Three representative prestack CDP gathers in which the reflections from the seafloor and BSR are identified are highlighted.
- Fig. 4. Illustration of peak frequency method for the CDP gathers from both the inline and crossline seismic profiles. The variation of peak frequency of BSR as a function of offset/time is shown for each CDPs. The seismic quality factor (Q) is estimated by minimizing the difference between the observed peak frequency and that predicted from peak-frequency method [equation (6)] using constrained non-linear optimization technique.
- Fig. 5 A) The variation in effective quality factor (Q) along the inline seismic profile. The estimated background Q-value is shown on the figure. B) The interpreted seismic section highlighting major features such as fault system (F1-F4), free gas bearing horizon and blanking zone in the study area.
- Fig. 6 A) The variation in effective quality factor (Q) along the crossline seismic profile. The estimated background Q-value is shown on the figure. B) The interpreted seismic section highlighting major fault system in the study area. C) The velocity model derived from the conventional semblance analysis (modified after Dewangan et al., 2011).
- Fig. 7. A) The effective Q^{-1} model estimated using peak frequency method along the seismic line; B) The interval velocity model estimated using full waveform inversion (Jaiswal et al., 2012b); C) The interval Q^{-1} model estimated using full-waveform inversion (Jaiswal et al., 2012b) using a starting model with zero attenuation.

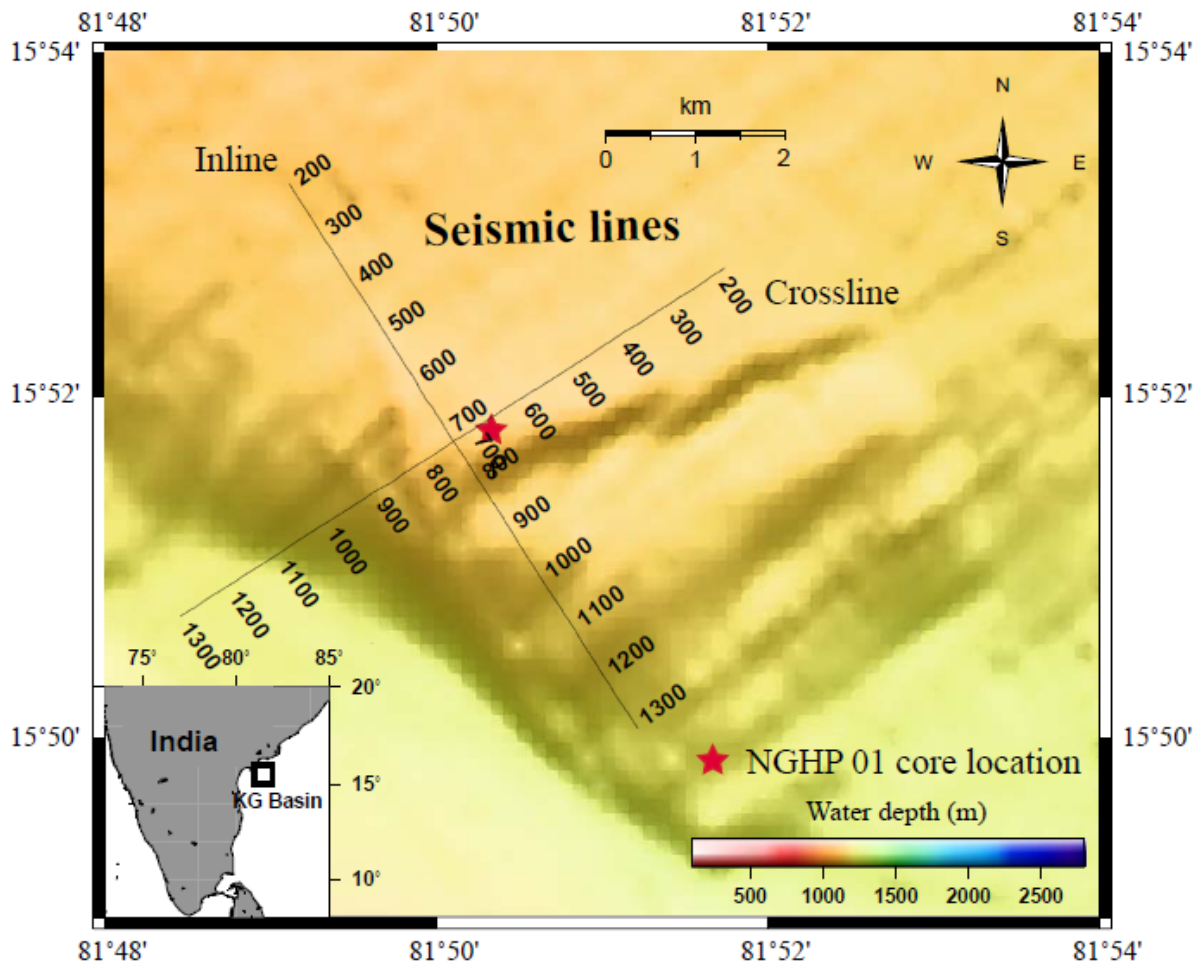


Figure 1

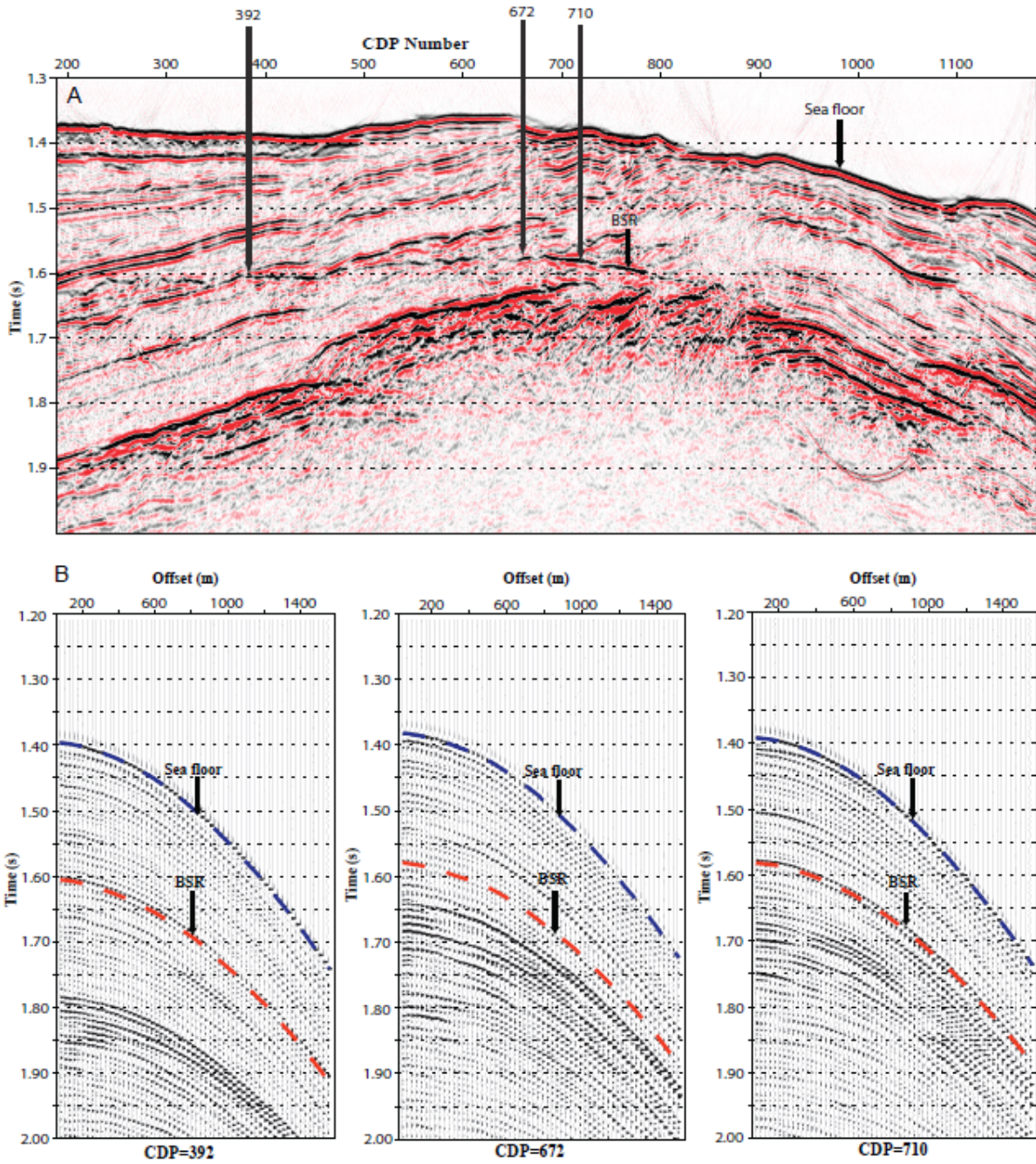


Figure 2

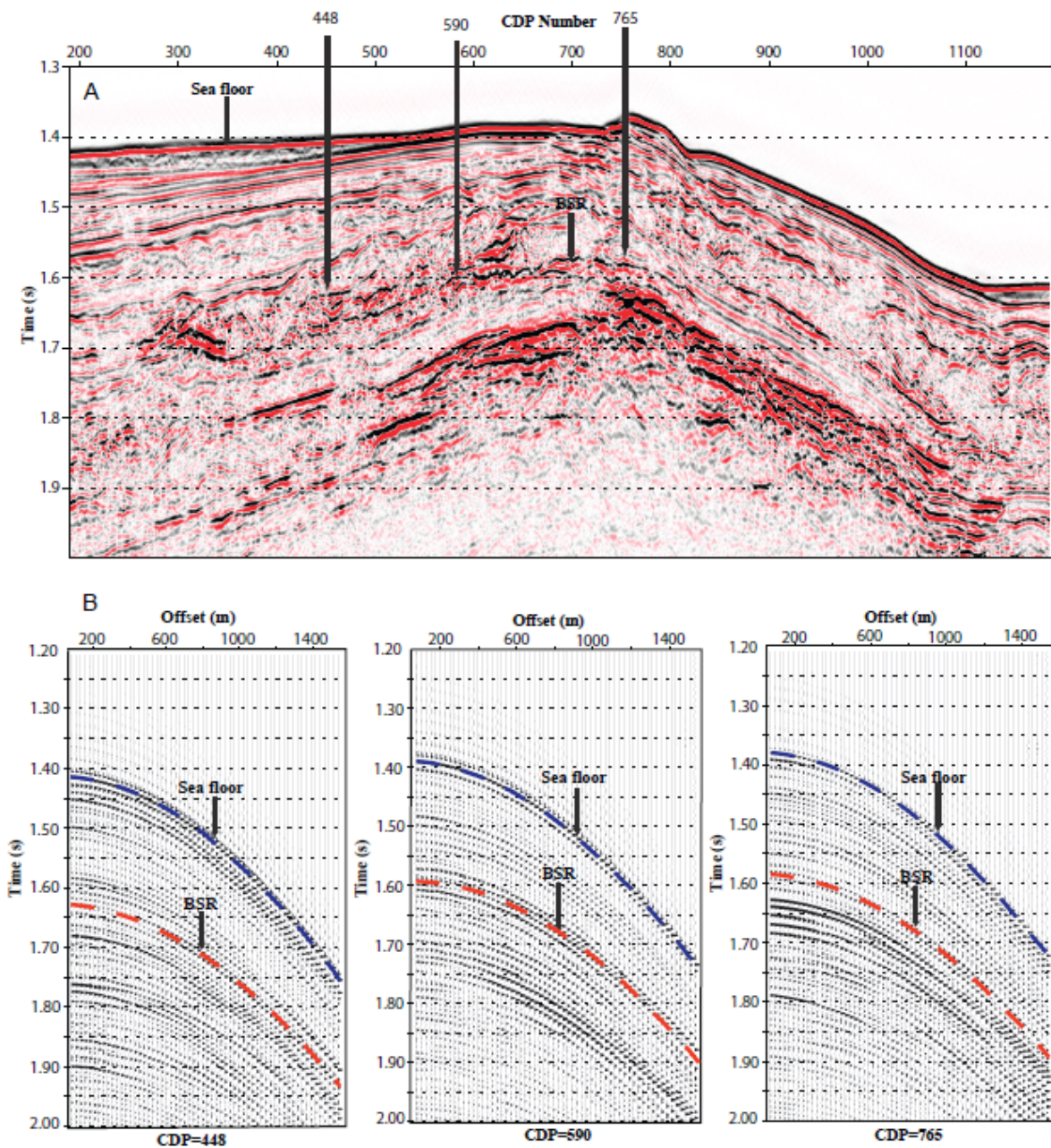


Figure 3

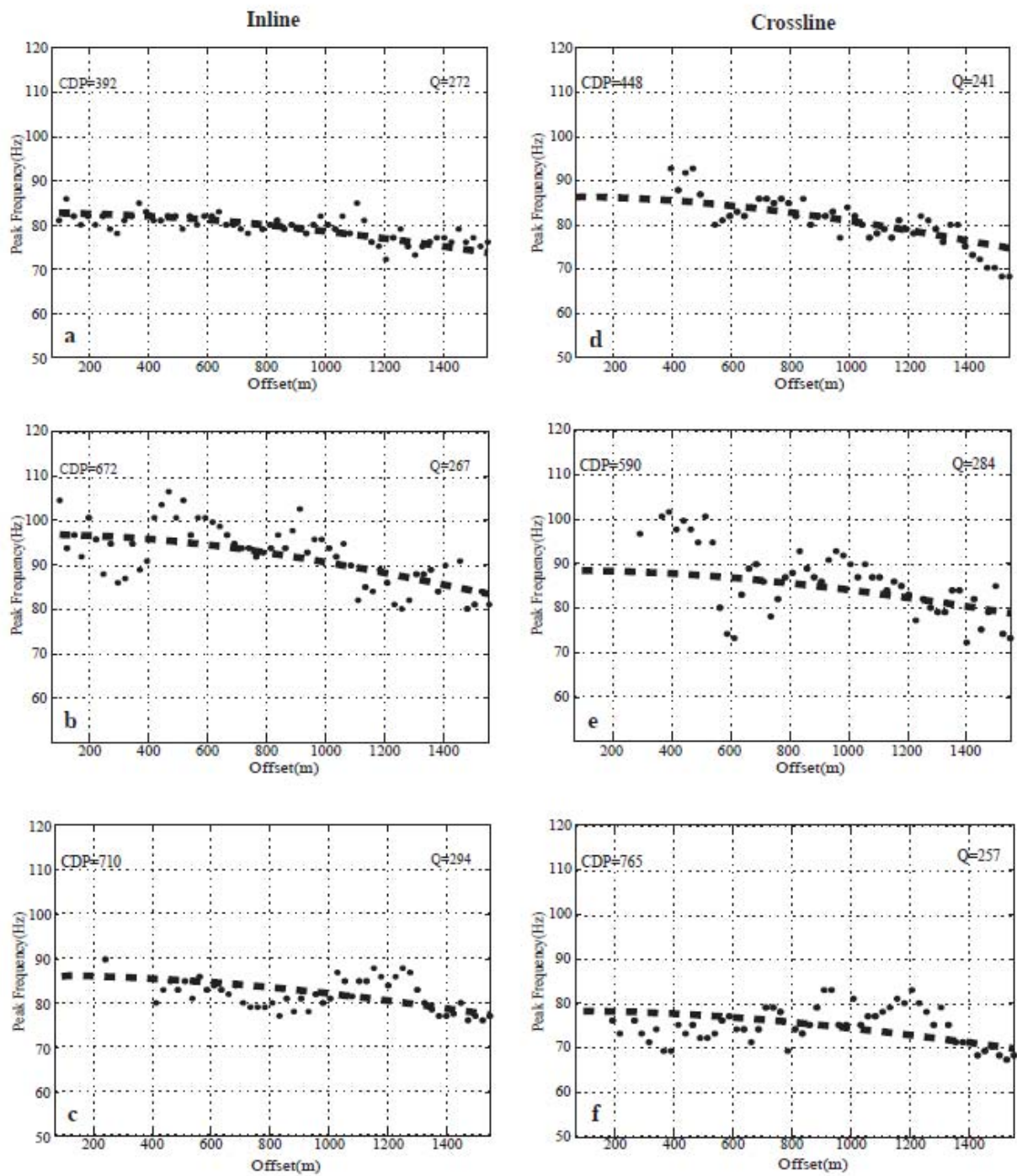


Figure 4

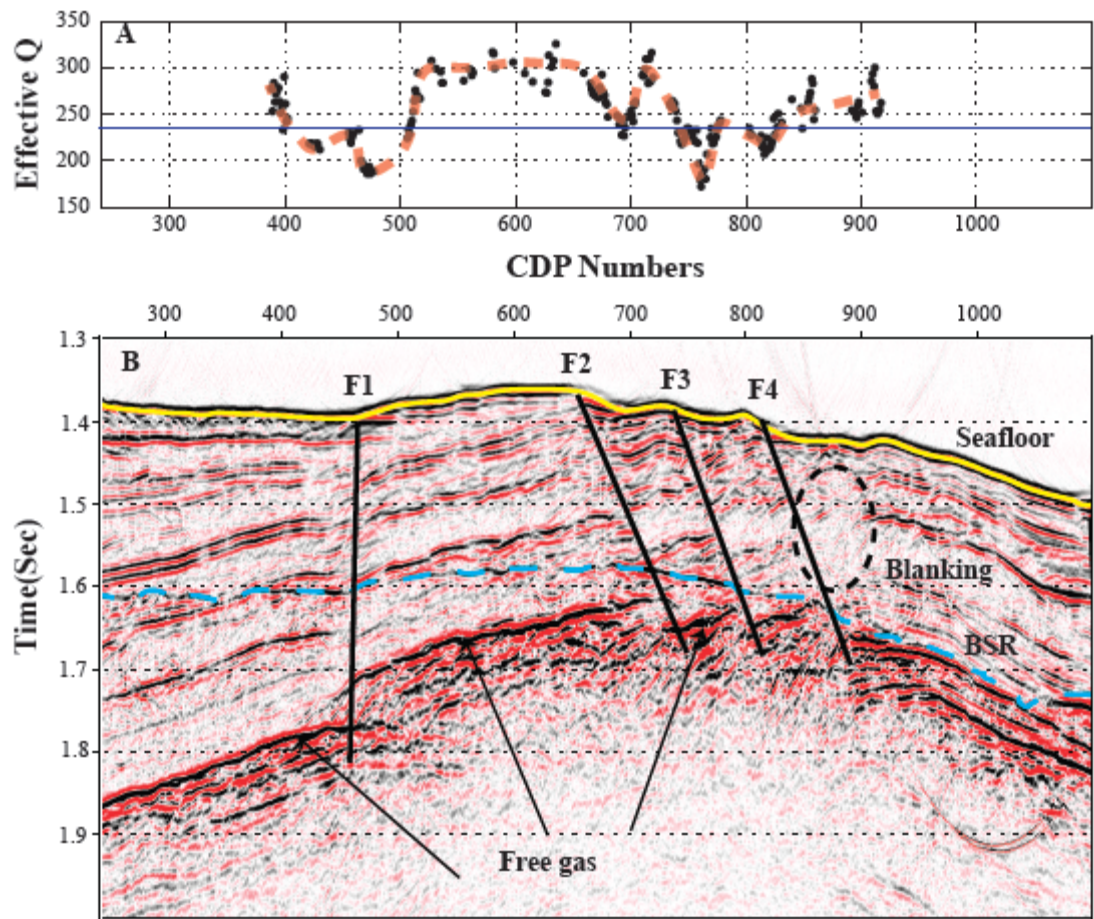


Figure 5

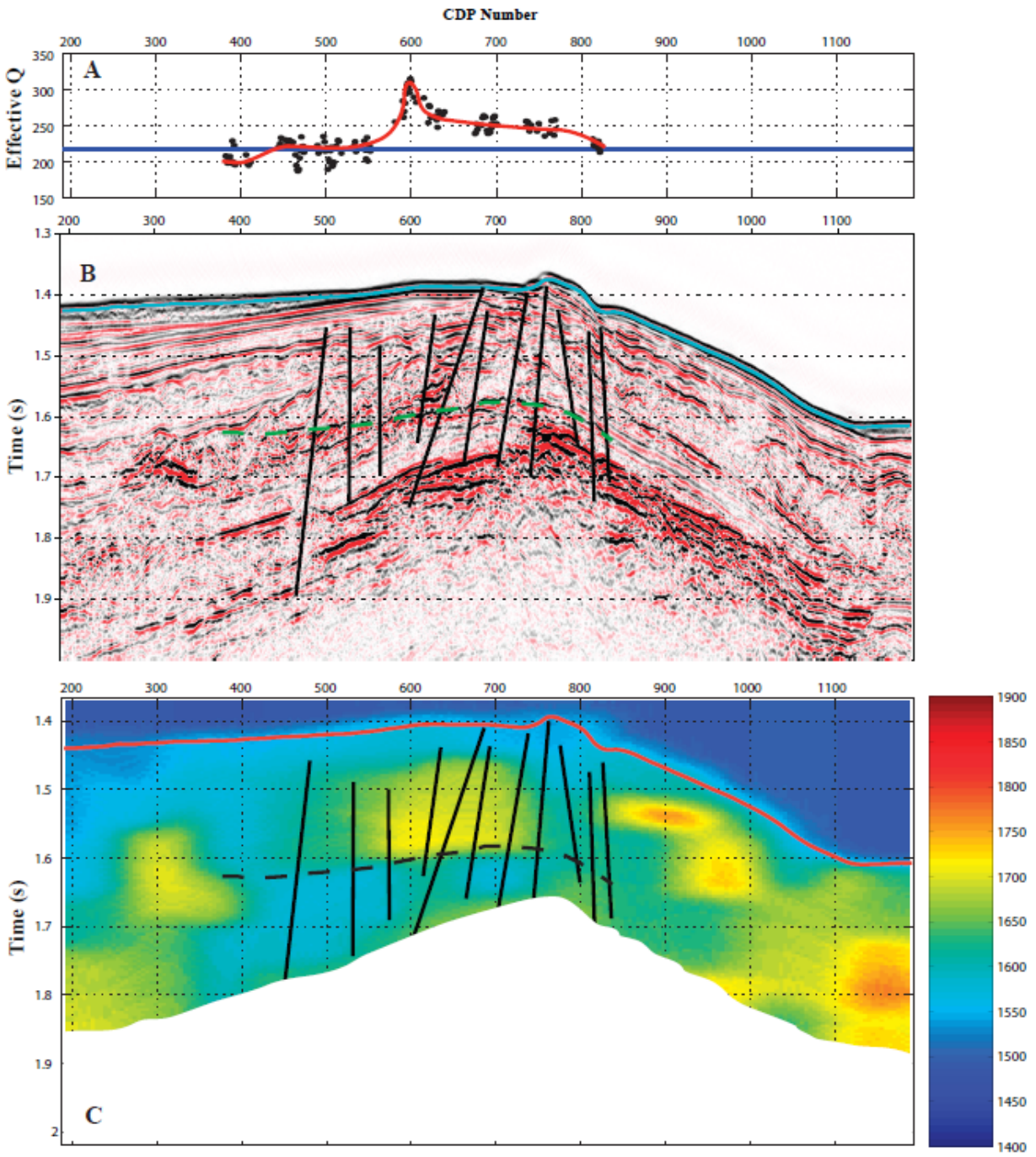


Figure 6

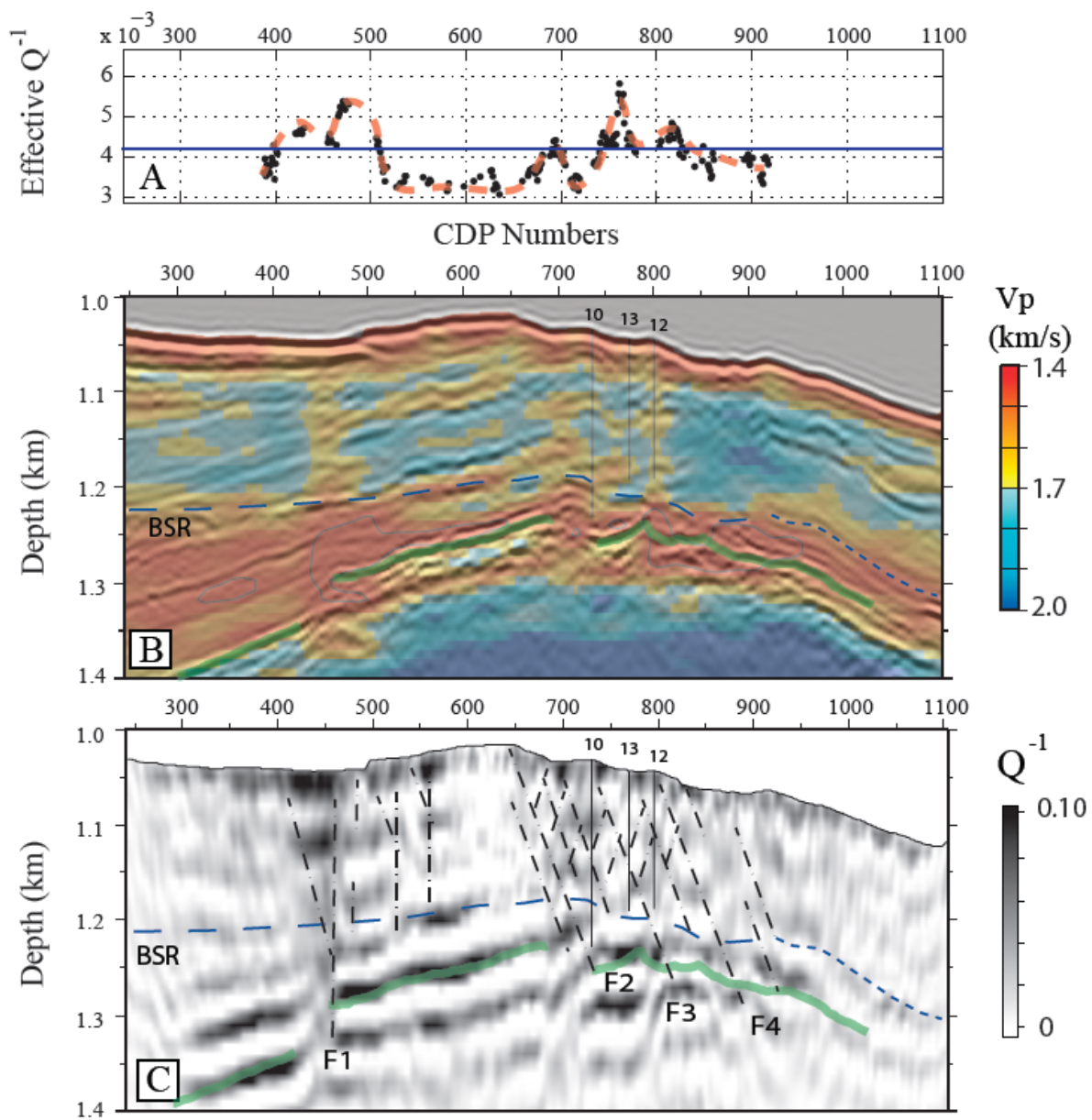


Figure 7